

Strong-disorder renormalization group study of the Anderson localization transition in three and higher dimensions

H. Javan Mard,¹ José A. Hoyos,² E. Miranda,³ and V. Dobrosavljević¹

¹*Department of Physics and National High Magnetic Field Laboratory, Florida State University, Tallahassee, FL 32306*

²*Instituto de Física de São Carlos, Universidade de São Paulo, C.P. 369, São Carlos, SP 13560-970, Brazil*

³*Instituto de Física Gleb Wataghin, Unicamp, R. Sérgio Buarque de Holanda, 777, Campinas, SP 13083-859, Brazil*

(Dated: August 20, 2021)

We implement an efficient strong-disorder renormalization-group (SDRG) procedure to study disordered tight-binding models in any dimension and on the Erdős–Rényi random graphs, which represent an appropriate infinite dimensional limit. Our SDRG algorithm is based on a judicious elimination of most (irrelevant) new bonds generated under RG. It yields excellent agreement with exact numerical results for universal properties at the critical point without significant increase of computer time, and confirm that, for Anderson localization, the upper critical dimension $d_{uc} = \infty$. We find excellent convergence of the relevant $1/d$ expansion down to $d = 2$, in contrast to the conventional $2 + \epsilon$ expansion, which has little to say about what happens in any $d > 3$. We show that the mysterious “mirror symmetry” of the conductance scaling function is a genuine strong-coupling effect, as speculated in early work [1]. This opens an efficient avenue to explore the critical properties of Anderson transition in the strong-coupling limit in high dimensions.

PACS numbers: 71.10.Fd, 71.23.An, 71.30.+h, 72.15.Rn

The Anderson transition is a nontrivial consequence of destructive interference effects in disordered materials. Its simplest realization is provided by the tight-binding model which describes electronic states in a “dirty” conductor by mimicking the effect of impurities through a random onsite potential. In spite of extensive studies, one easily finds that some basic questions remain unanswered or in disagreement. For instance, different values of the upper critical dimension $d_u = 4, 6,$ and 8 [2–6] and $d_u = \infty$ [7–9] have been reported. This question may look like purely academic but indeed it has practical applications in quantum kicked rotor systems [10] where the effective dimensionality of the dynamical localization is determined by the number of incommensurate frequencies in the system. [11]

One main challenge in investigating the localization transition is the limited range of applicability of well known analytical approaches. For example, The traditional “weak-localization” approach to the Anderson metal-insulator transition is based on the fact that, in the vicinity of the $d=2$, the transition is found at weak disorder, where perturbative methods can be used; this lead to a flurry of results in 1980s. On the other hand, more recent numerical results demonstrated that predictions from such $2+\epsilon$ expansions provide poor guidance even in $d=3$, similarly as in other theories starting from the lower critical dimension. [12–16] In contrast, the progress in numerical calculations during the last 20 years has increased dramatically our knowledge of the metal-insulator transition, especially in dimensions such as $d = 3$ and 4 for which a rigorous analytical treatment is not available.

For most critical phenomena, the upper critical dimension has provided a much better starting point, but so far

such an approach has not been available for Anderson localization. Since in high dimensions the Anderson point shifts away from weak disorder, an appropriate strong-disorder approach is called for. Here we show how an accurate Strong Disorder Renormalization Group (SDRG) approach can be developed for Anderson localization, where quantitatively accurate results can be obtained in all dimensions. The SDRG method has been successful in describing the critical and near-critical behavior of the Random Transverse-Field Ising model and other random magnetic transitions, [17, 18] and have been recently used in electronic systems. [19, 20]

Avoiding finite-size effects by having access to very large system sizes and flexibility to work in any dimensions or topology in reasonable time and computer memory resources have been always a long lived goal for computational physicists. In this letter, we achieved this goal by designing an efficient numerical approach able to study the localization transition in the tight-binding model by computing the conductance in all dimensions without much effort. Our implementation of the method only keeps track of the main couplings in the system which allowed us to greatly speed up the computer time.

Model and method.— We study the d -dimensional tight-binding model

$$H = - \sum_{i,j} (t_{i,j} c_i^\dagger c_j + \text{h.c.}) + \sum_i \varepsilon_i c_i^\dagger c_i, \quad (1)$$

where $c_i^\dagger (c_i)$ is the canonical creation (annihilation) operator of spineless fermions at site i , $t_{i,j} = t_{j,i}$ is the hopping amplitude between sites i and j , and ε_i is the onsite energy. The site energies ε_i are identically distributed random variables drawn from a uniform distri-

bution of zero mean and width W , and the hopping amplitude $t_{i,j} = 1$ if sites i and j are connected (which is model dependent), otherwise it is zero. We treat this model using the SDRG method [20] and compute the dimensionless conductance defined as

$$g \equiv g_{\text{typ}} = \frac{\langle T \rangle_{\text{geo}}}{1 - \langle T \rangle_{\text{geo}}} \quad (2)$$

where T is the transmittance, and $\langle \dots \rangle_{\text{geo}}$ denotes the geometric average. In this work, we will consider only leads that are connected to single sites of the sample. Therefore, g is the two-point conductance.

The SDRG method consists in a iterative elimination of the strongest energy scale $\Omega = \max\{|\varepsilon_i|, |t_{ij}|\}$ (with the exception of those connected to the external wires) and renormalizing the remaining ones couplings in the following fashion: (i) if $\Omega = |\varepsilon_i|$, then site i is eliminated from the system and the remaining couplings are renormalized to

$$\tilde{\varepsilon}_k = \varepsilon_k - \frac{t_{i,k}^2}{\varepsilon_i}, \quad (3)$$

and

$$\tilde{t}_{k,l} = t_{k,l} - \frac{t_{k,i}t_{i,l}}{\varepsilon_i}, \quad (4)$$

on the other hand if (ii) $\Omega = |t_{i,j}|$, then sites i and j are eliminated from the system yielding the renormalized couplings

$$\tilde{\varepsilon}_k = \varepsilon_k - \frac{\varepsilon_i t_{i,k}^2 - 2t_{i,j}t_{i,k}t_{j,k} + \varepsilon_j t_{j,k}^2}{t_{i,j}^2 - \varepsilon_i \varepsilon_j}, \quad (5)$$

and

$$\tilde{t}_{k,l} = t_{k,l} + \frac{\varepsilon_j t_{i,k}t_{i,l} - t_{i,j}(t_{i,k}t_{j,l} + t_{i,l}t_{j,k}) + \varepsilon_i t_{j,k}t_{j,l}}{t_{i,j}^2 - \varepsilon_i \varepsilon_j}. \quad (6)$$

In this way, we eliminate all the sites until there is a single renormalized coupling $\tilde{\varepsilon}_\alpha$ - $\tilde{t}_{\alpha,\beta}$ - $\tilde{\varepsilon}_\beta$ connecting the leads at sites α and β from which the transmittance T can be computed straightforwardly.

These transformations, although computed in perturbation theory, are *exact* in the purpose of studying transport properties (transmittance) since it preserves the Green's function. [21] As a consequence, this method yields accurate results for the critical parameters associated with the localization transition in any dimensions. However, as can be seen from Eqs. (3)–(6), the reconnection of the lattice requires an increasing amount of memory and the procedure becomes unpractical. In order to avoid this problem, many schemes were proposed which are model dependent. [22–24] The modification of

the SDRG scheme we adopt in this work is setting a maximum coordination number k_{max} per site, i.e., we follow the exact SDRG procedure but only keep track of the strongest k_{max} couplings in each site. A detailed study comparing the “exact” and “modified” SDRG procedures will be given elsewhere. [25]

Infinite dimensional limit.—In Erdős–Rényi (ER) random graph, we consider a system of $N \gg 1$ sites in which two given sites i and j are connected with probability p ($t_{i,j} = 1$) and disconnected with probability $1 - p$ ($t_{i,j} = 0$). Since the average number of sites at a “distance” L from a particular site increases exponentially with L , it effectively corresponds to the limit of $d \rightarrow \infty$.

In order to have a well defined length scale, the contact leads are attached to two sites at the average shortest distance L_{ER} , where $L_{\text{ER}} = \ln N / \ln \langle k \rangle$. [26] Here, $\langle k \rangle = p(N - 1)$ is the average coordination number which is chosen to be greater than the percolation threshold $k_c = 1$. [27] We verified that our final results do not depend on the exact value of $\langle k \rangle$ as long as it is near and above k_c .

In similarity with previous studies on the Bethe lattice, [28] the distinction between the conducting and insulating phases manifests in the different behavior of the “weighted” two-point conductance $g_w(L) = N(L)g$. The extra factor $N(L) = \langle k \rangle (\langle k \rangle - 1)^{L-1}$ counts the number of sites located at the distance L from a given site. It does not play any significant role in the universal behavior of conductance [see Figs. 1(a) and (b)] but is useful to pinpoint the critical point W_c [see inset of Fig. 1(a)] and to obtain the localization length ξ in the localized phase: $\ln g_w \sim -L/\xi$. The critical disorder value $W_c = 14.5(3)$ (exact SDRG) and $W_c = 13.0(3)$ (modified SDRG with $k_{\text{max}} = 20$). Our estimate for the localization length exponent (defined via $\xi \sim |W - W_c|^{-\nu}$ considering only ξ that are less than L_{ER}) is $\nu = 0.98(4)$ (exact SDRG) and $\nu = 1.01(5)$ (modified SDRG) which is very close to the exact value $\nu = 1$ in $d \rightarrow \infty$. [28, 29] In the metallic phase, the localization length is obtained by dividing L by ξ such that all the curves g_w/g_{wc} collapse in a single curve. This procedure is precise up to an irrelevant global pre-factor. In this way, we confirm that ν is the same in both localized and delocalized phases (within the statistical error).

Cubic lattice in $d = 3$.—We now apply the SDRG method to the cubic lattice in $d = 3$. Here, $t_{i,j} = 1$ if i and j are nearest neighbors, and $t_{i,j} = 0$ otherwise. The value of upper cutoff k_{max} can be adjusted according to desired accuracy. Here, as in the ER graph, a modest value of $k_{\text{max}} = 20$ is sufficient for getting good agreement between the exact and modified SDRG methods (within the 5% of the statistical accuracy). We have used chains of sizes $L = 8, 10, 12, 15$, and 20 with periodic boundary conditions and the leads were attached to the corner and to the center sites of the sample (maximum possible distance). In the inset of Fig. 2(a), we

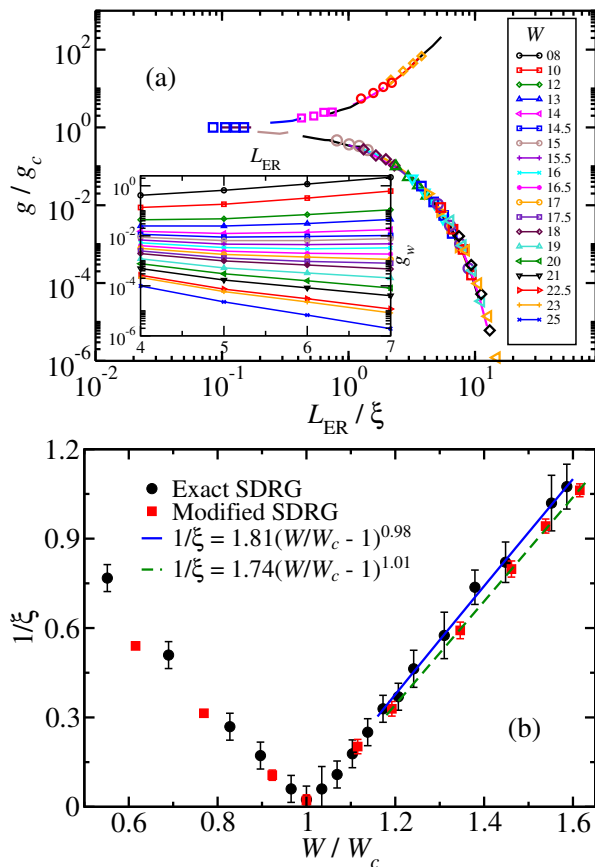


Figure 1. (a) The typical two-point conductance g of the ER random graph with $\langle k \rangle = 3.0$ and $N = 3^{L_{ER}}$, $L_{ER} = 4, \dots, 7$ for several disorder parameters $W = 8$ up to $W = 25$ using the exact SDRG procedure (colorful solid lines) and our modified algorithm (colorful symbols). We average over as many disorder realizations needed to reach 5% of precision (see main text for details). Inset: the weighted conductance g_w as a function of L_{ER} . Legends correspond to the inset, not the main panel. (b) The localization length near the localization transition.

plot $g_w = L^3 g$ for various disorder parameter W . Unlike the ER graph, it is not so simple to pinpoint the critical point W_c , mainly because g_w at criticality is not constant for large L . We then try scaling using different critical W_c until the best data collapse is obtained [see Fig. 2(a)]. We find $W_c = 16.5(5)$ (exact SDRG) and $W_c = 17.5(5)$ (modified SDRG). The localization length exponent is obtained in the same way as in the ER graph [see Fig. 2(b)] from which we obtained $\nu = 1.57(1)$ in agreement with previous results. [30, 31] Although this result is obtained by fitting only those data in which $\xi < 20$, it fits quite well all the entire data set.

Figure 3 presents a study of dimensional dependency of ν at $d = 3, 4, 6, 10$, and infinity using different approaches. It manifests the limited range of applicability of some well-known analytical theories such as $2 + \epsilon$ expansion, the self-consistent theory proposed by D. Voll-

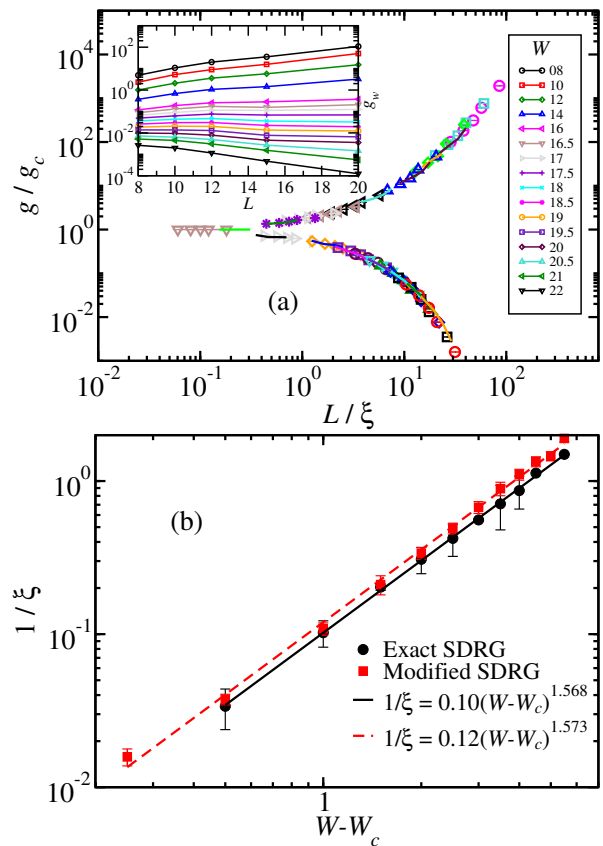


Figure 2. (a) The typical two-point conductance g for the 3D cubic lattice for various disorder parameters using the exact SDRG procedure (colorful solid lines) and our proposed modified algorithm (colorful symbols). Inset: the weighted two-point conductance g_w obtained from the exact SDRG method. Legends correspond to the inset, not the main panel. (b) The localization length ξ (in the localized phase) as a function of the distance from criticality $W - W_c$.

hardt and P. Wölfle, and phenomenological proposal of the beta function in $d \geq 1$ by Shapiro's work. They lead to very poor results for ν as d becomes equal or higher than 3. Our modified SDRG algorithm estimations for ν are consistent with the most recent numerical computation done by Y. Ueoka and K. Slevin on dimensions up to 5. [32] It is clear from our data, the upper critical dimension is not at finite dimensions predicted in references [2–6] while infinite dimension seems more reasonable candidate for the upper critical dimension of Anderson model. In contrast to García-García work, we find $1/\nu$ follows a behavior more complicated than a linear relationship with $1/d$ (a cubic function fits well with our data points in Fig. 3). Our modified algorithm allows us to study higher dimensions without limiting us to very small system sizes which provides us a better prediction for the behavior described in Fig. 3.

In contrast to weak disorder approach, our approach based on strong disorder limit presents much more reasonable results in estimating the critical exponent for

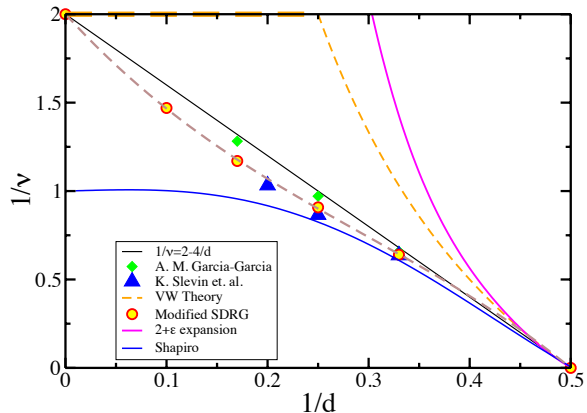


Figure 3. The inverse of critical exponent ν is plotted versus $1/d$ for $d \geq 2$, along with some recent numerical estimations of this exponent in higher dimensions by Slevin et. al. [32] (Blue triangles) and García-García [9] (Green diamonds). Analytical predictions of three well-known theories are included to stress the limited range of reliability of them to estimate ν as it is discussed in the main text. The Brown color dashed line is a cubic function fitted to our data presenting the number of orders of $1/d$ needed to describe the localization transition for $d \geq 2$. The coefficients of cubic fitted function are computed as $c_0 = 2.000 \pm 0.008$, $c_1 = -6.263 \pm 0.167$, $c_2 = 10.380 \pm 0.864$, and $c_3 = -11.713 \pm 1.1458$, respectively.

$d \geq 3$. The significant role of strong coupling in localization transition is also prominent in study of the mirror symmetry phenomena which has been also observed experimentally. [33, 34] The Mirror Symmetry Range (MSR) can be defined as the range of g/g_c where mirror symmetry in the scaling function holds. The mirror symmetry idea was proposed in early work for two dimensional MIT, where they conclude that the related experimental results provide striking evidence about the form of the beta function in the critical region. [1] In particular, they indicate that in a wide range of conductances the beta function is well-approximated by the linear expression in $t = \ln(g/g_c)$. This observation can be interpreted by noticing that deep in the insulating regime, ($g \ll g_c$) the beta function is exactly given by $\beta(g) \sim \ln(g)$. The related experimental result can thus be interpreted as evidence that the same slow logarithmic form of the beta function persists beyond the insulating limit well into the critical regime. This feature could be used as a basis of approximate calculations of the critical exponents. In contrast to the well-known $2 + \epsilon$ expansion, here one would try to obtain the form of the beta function in the critical region by an expansion around the strong disorder limit.

Applications.—Since the number of sites increases rapidly with lattice size in higher dimensions, depending on accessible computer memory, one might be limited to

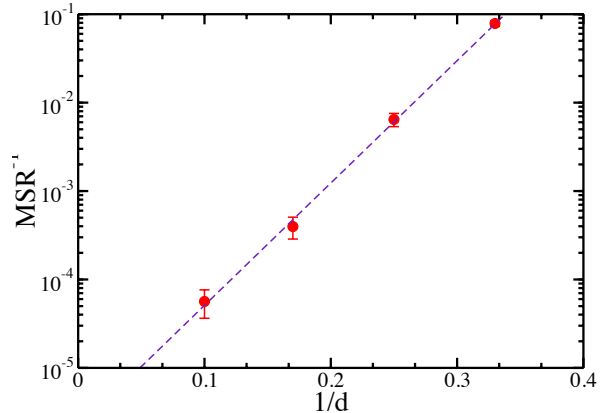


Figure 4. The inverse of Mirror Symmetry Range (MSR) as a function of $1/d$ presents an increasing trend implying the strong-coupling effect. The dashed line presents the fitting function expressed as $MSR^{-1} = a \exp(b/d)$ where $a = 2.10 \times 10^{-6}$ and $b = 31.86 \pm 0.88$.

try arbitrary large system size. In this situation, an alternative solution is to use a site percolated hyper-cubic lattice instead, to decrease the number of sites which actually play important role in the transition (We expect the critical behavior does not vary with $\langle k \rangle$ as long as it is above its classical percolation threshold.). Another possible application of our method is to consider the global conductance instead of the two-point one. In this case, the leads will be attached to opposite planes of the sample which will be fully connected after the interior is decimated out.

Conclusion.—We showed our modified SDRG method is suitable to study the localization properties of large system in any dimension. This significant progress eliminates previous obstacles such as computational time or computer memory size and paves the avenue for future study of the Anderson transition. We provided concluding evidence that the upper critical dimension for localization is infinity. Considering neither the self-consistent theory of localization exact for the Cayley tree nor the ϵ -expansion formalism is accurate for intermediate dimensions, we proposed a strong coupling basis for the localization problem and infinite dimension as starting point.

This work was supported by the NSF grants DMR-1005751, DMR-1410132 and PHYS-1066293, by the National High Magnetic Field Laboratory, by the Simons Foundation, by FAPESP under Grants 07/57630-5 and 2013/09850-7, and by CNPq under Grants 304311/2010-3, 590093/2011-8 and 305261/2012-6. We acknowledge the hospitality of the Aspen Center for Physics.

-
- [1] V. Dobrosavljević, E. Abrahams, E. Miranda, and S. Chakravarty, Phys. Rev. Lett. **79**, 455 (1997).
- [2] D. J. Thouless, Journal of Physics C: Solid State Physics **9**, L603 (1976).
- [3] T. Lukes, Journal of Physics C: Solid State Physics **12**, L797 (1979).
- [4] A. Harris and T. Lubensky, Phys. Rev. B **23**, 2640 (1981).
- [5] J. Straley, Phys. Rev. B **28**, 5393 (1983).
- [6] I. Suslov, Journal of Experimental and Theoretical Physics Letters **63**, 895 (1996).
- [7] A. Mirlin and Y. Fyodorov, Phys. Rev. Lett. **72**, 526 (1994).
- [8] C. Castellani, C. D. Castro, and L. Peliti, Journal of Physics A: Mathematical and General **19**, L1099 (1986).
- [9] A. M. García-García and E. Cuevas, Phys. Rev. B **75**, 174203 (2007).
- [10] F. Moore, J. Robinson, C. Bharucha, B. Sundaram, and M. Raizen, Phys. Rev. Lett. **75**, 4598 (1995).
- [11] G. Casati, I. Guarneri, and D. Shepelyansky, Phys. Rev. Lett. **62**, 345 (1989).
- [12] F. Wegner, Zeitschrift für Physik B Condensed Matter **36**, 209 (1980).
- [13] F. Wegner, Zeitschrift für Physik B Condensed Matter **25**, 327 (1976).
- [14] D. Vollhardt and P. Wölfle, Phys. Rev. Lett. **48**, 699 (1982).
- [15] M. Schreiber and H. Grussbach, Phys. Rev. Lett. **76**, 1687 (1996).
- [16] B. K. I. Kh. Zharekeshev, Ann. Phys. (Leipzig) **7**, 442 (1998).
- [17] D. S. Fisher, Phys. Rev. Lett. **69**, 534 (1992).
- [18] F. Iglói and C. Monthus, Phys. Rep. **412**, 277 (2005).
- [19] C. Monthus and T. Garel, Phys. Rev. B **80**, 024203 (2009).
- [20] H. Javan Mard, J. A. Hoyos, E. Miranda, and V. Dobrosavljević, Phys. Rev. B **90**, 125141 (2014).
- [21] H. Aoki, Journal of Physics C: Solid State Physics **13**, 3369 (1980).
- [22] O. Motrunich, S.-C. Mau, D. A. Huse, and D. S. Fisher, Phys. Rev. B **61**, 1160 (2000).
- [23] J. A. Hoyos and E. Miranda, Phys. Rev. B **69**, 214411 (2004).
- [24] I. A. Kovács and F. Iglói, Phys. Rev. B **83**, 174207 (2011).
- [25] H. Javan Mard, J. A. Hoyos, E. Miranda, and V. Dobrosavljević, Unpublished.
- [26] A. Fronczak, P. Fronczak, and J. A. Holyst, Phys. Rev. E **70**, 56110 (2004).
- [27] R. V. Sole, *Phase transitions* (Princeton University Press, 2011).
- [28] A. D. Mirlin and Y. V. Fyodorov, Nuclear Physics B **366**, 507 (1991).
- [29] C. Monthus and T. Garel, Journal of Physics A: Mathematical and Theoretical **42**, 075002 (2009).
- [30] K. Slevin and T. Ohtsuki, Phys. Rev. Lett. **82**, 382 (1999).
- [31] A. Rodriguez, L. Vasquez, K. Slevin, and R. Römer, Phys. Rev. B **84**, 134209 (2011).
- [32] Y. Ueoka and K. Slevin, Journal of the Physical Society of Japan **83**, 084711 (2014), <http://dx.doi.org/10.7566/JPSJ.83.084711>.
- [33] S.-Y. Hsu and J. M. Valles, Jr., Phys. Rev. Lett. **74**, 2331 (1995).
- [34] S. V. Kravchenko, D. Simonian, M. P. Sarachik, W. Mason, and J. E. Furneaux, Phys. Rev. Lett. **77**, 4938 (1996).

Supplemental notes for: “Strong-disorder renormalization group study of the Anderson localization transition in three and higher dimensions”

H. Javan Mard,¹ José A. Hoyos,² E. Miranda,³ and V. Dobrosavljević¹

¹*Department of Physics and National High Magnetic Field Laboratory, Florida State University, Tallahassee, FL 32306*

²*Instituto de Física de São Carlos, Universidade de São Paulo, C.P. 369, São Carlos, SP 13560-970, Brazil*

³*Instituto de Física Gleb Wataghin, Unicamp, R. Sérgio Buarque de Holanda, 777, Campinas, SP 13083-859, Brazil*

(Dated: August 20, 2021)

PACS numbers:

I. SDRG APPROACH COMPUTES THE CONDUCTANCE EXACTLY

It is easy to prove that the SDRG transformations derived in our previous work leads to compute the exact two point conductance in the Anderson model. If we integrate out a site, say m , during SDRG process while keeping the Green's function conserved between two arbitrary sites i , and j :

$$G(i, j) = \frac{1}{Z} \int D[\phi_k(\tau), \phi_k^*(\tau)] \phi_i(\tau) \phi_j(\tau) e^{-S[\phi_k(\tau), \phi_k^*(\tau)]}, \quad (1)$$

where

$$D[\phi_k(\tau), \phi_k^*(\tau)] = \prod_{k=1}^n d\phi_k(\tau) d\phi_k^*(\tau),$$

and

$$S[\phi_k(\tau), \phi_k^*(\tau)] = - \int_0^\beta d\tau \left[\sum_k \phi_k^*(\tau) \left\{ \frac{\partial}{\partial \tau} - \mu + \varepsilon_k \right\} \phi_k(\tau) + \sum_{k,l} \phi_k^* t_{kl} \phi_l \right]. \quad (2)$$

Using the frequency representation,

$$S[\phi_k(\omega), \phi_k^*(\omega)] = - \left[\sum_{k,n} \phi_k^*(\omega_n) \{i\omega_n - \mu + \varepsilon_k\} \phi_k(\omega_n) + \sum_{k,l} \phi_k^*(\omega_n) t_{kl} \phi_l(\omega_n) \right]. \quad (3)$$

At $\omega = \mu = 0$, we can simplify the above equation to $S = -[\sum_k \phi_k^* \{\varepsilon_k\} \phi_k + \sum_{k,l} (\phi_k^* t_{kl} \phi_l + h.c.)]$. Then, those terms in S associated to m can be rewrite as:

$$-\phi_m^* \varepsilon_m \phi_m - \sum_k (\phi_m^* t_{mk} \phi_k + h.c.) = -\varepsilon_m \left[(\phi_m^* + \sum_k \frac{t_{mk}}{\varepsilon_m} \phi_k^*) (\phi_m + \sum_k \frac{t_{mk}}{\varepsilon_m} \phi_k) \right] + \sum_{kl} \phi_k^* \frac{t_{mk} t_{ml}}{\varepsilon_m} \phi_l \quad (4)$$

The first term in Eq. 4 will be canceled out by doing the same calculation in denominator of $G(i, j)$ (we assume ε_m is nonzero.), but the second term leads to renormalize the hopping term between sites k and l :

$$\tilde{t}_{kl} = t_{kl} - \frac{t_{mk} t_{ml}}{\varepsilon_m} \quad (5)$$

This is the same decimation rules for ε , and t -decimations of our SDRG approach.

How about t-decimations?

Decimation of a bond also can be described as integrating out its two neighbor sites one by one in the purpose of conservation of two point Green's function. For example, assume we first integrate out the site 2 and then site 3. After first decimation, we have

$$\tilde{t}_{kl} = t_{kl} - \frac{t_{2k} t_{2l}}{\varepsilon_2}$$

then by decimating the site 3,

$$\begin{aligned} \tilde{\tilde{t}}_{kl} &= \tilde{t}_{kl} - \frac{\tilde{t}_{3k} \tilde{t}_{3l}}{\tilde{\varepsilon}_3} = t_{kl} - \frac{t_{2k} t_{2l}}{\varepsilon_2} - \frac{(t_{3k} - \frac{t_{23} t_{2k}}{\varepsilon_2})(t_{3l} - \frac{t_{23} t_{2l}}{\varepsilon_2})}{\varepsilon_3 - \frac{t_{23}^2}{\varepsilon_2}} \\ &= t_{kl} + \frac{\varepsilon_3 t_{2k} t_{2l} + t_{23}(t_{2k} t_{3l} + t_{2l} t_{3k}) + \varepsilon_2 t_{3k} t_{3l}}{t_{23}^2 - \varepsilon_2 \varepsilon_3}. \end{aligned}$$

This is exactly what we use as SDRG decimation rules for any dimensions.

II. THE MODIFIED SDRG ALGORITHM

1- N energy sites are randomly chosen from a uniform distribution. In the case of ER random graph, two sites are connected with a probability less than $p = \langle k \rangle / (n - 1)$, thus we can generate a graph either by checking this condition for each pair of sites or by randomly choosing $m = pn$ of pairs of sites. The latter method is useful specially for very large n . Since we only keep k_{max} bonds per site, the required memory space is $k_{max} n$ and it takes $\mathcal{O}(mn)$ to create the Hamiltonian matrix. We recall that $m \ll n$ for a sparse graph.

2- In the case of ER random graph, we use Dijkstra algorithm to find the shortest path between sites, but only those sites that they have a relative distance $l_{ER} = \ln(N)/\ln(\langle k \rangle)$ will be chosen to be attached to the leads. The worst running time of this algorithm is known $\mathcal{O}(m \log n)$ to determine all shortest paths from one reference site. Moreover, above the percolation threshold, we are only interested in the giant component of graph and one can ignore sites excluded from this component (doing that decrease the number of considered sites by almost %5 in ER graph with $\langle k \rangle = 3$ which is large number when n is very large.).

3-Decimation process: We search for the maximum of $\{\varepsilon_i, t(i, j)\}$, and decimate them as it is explained in the main text. Performing a SDRG decimation causes the adjacency list shrinks at least by one site in each step, and gives a faster running time for the rest of code in return. It is important that the sites attached to the leads, and their bonds will not be decimated during SDRG decimation, but their value still can be updated if a decimation happens in their neighbor.

Decimation of n sites consists of two parts:

3-1 Search for the maximum of energy terms: This will take $\mathcal{O}(\log n)$ if one use the Heap data structure to sort ε_i and t_{ij} values separately (More details on heap data structure, and its implementation in C++ programming language can be found in many books such as an interesting book written by Mark A. Weiss [1]).

3-2 Renormalization the neighbors: the number of neighbors are limited to k_{max} so there are k_{max} onsite energies and k_{max}^2 hopping terms: $\mathcal{O}(k_{max}^2 \log n)$

4- After decimating a site or bond if the coordination number of a particular site say j , exceeds k_{max} , we replace the weakest bond of site j with the new bond, otherwise we ignore it.

Therefore, the total running time of steps 1-4 would be $\mathcal{O}(n \log n)$.

5- Steps 1-4 can be repeated for different realization of initial disorder until achieving the desired accuracy.

Fig. 3 presents the efficiency of SDRG modified algorithm used for a 3D lattice in a range of system sizes accessible for all methods.

III. COMPUTATION OF CRITICAL EXPONENT ν IN $d > 3$

As we discussed earlier, the modified SDRG algorithm only depends on the number of sites in the lattice. Therefore, it is possible to take advantage of this method and compute ν in higher dimensions. However, the number of sites in higher dimensions grows faster with the lattice size and one should be concerned about the accessible computer memory and time, and the effect of k_{max} when it gets closer to the initial coordination number.

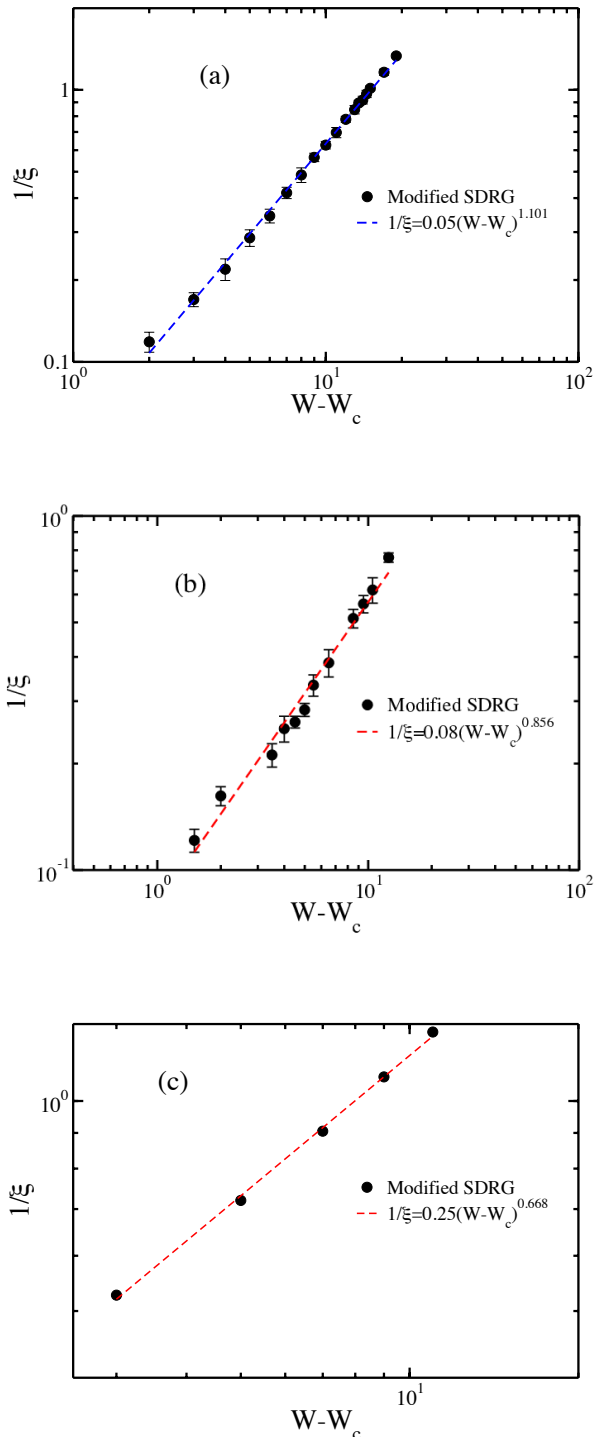


Figure 1: The critical exponent of the localization length is computed for a hyper-cubic lattice with $d = 4, 6,$ and 10 . (a) The critical exponent ν estimated as $\nu_{4D} = 1.10 \pm 0.09$ and $W_c = 22 \pm 0.5$. Here, we studied the disorder strength from 5 to 41, and system sizes $L = 6, 8, 10,$ and 12 . (b) In six dimension, the critical exponent computed as $\nu_{6D} = 0.86$ and $W_c = 51.5 \pm 0.5$. Here, W was changed from 20 to 70 and L from 6 to 12. (c) In 10D lattice, we used system sizes $L = 3, 4, 5$ and disorder strength from 80t to 110t. Our studies shows $W_c = 97 \pm 0.5$ and $\nu_{10D} = 0.68 \pm 0.06$.

IV. MIRROR SYMMETRY ANALYSIS:

The Mirror Symmetry Range (MSR) is defined as the range of g/g_c where mirror symmetry holds. Although this range can be simply estimated approximately just by looking or inverting the scaling function in one phase onto another one, but we measure MSR in a more well-defined approach as follows:

1-We plot $t = \ln(g/g_c)$ versus $y = \pm x^{1/\nu}$ where $x = L/\xi$ where the plus sign corresponds to the localized phase and the minus to the delocalized phase. Let's call the resulting function $t(y)$.

2- In the presence of symmetry, $t(y)$ is an odd function. Thus, we separate the odd and even parts of function $t(y)$ and find where the even part value becomes significant. In other words,

$$t_{odd}(y) = \frac{1}{2}[t(y) - t(-y)], \quad t_{even}(y) = \frac{1}{2}[t(y) + t(-y)] \quad (6)$$

$$t_{even}(y^*) = \alpha t_{odd}(y^*),$$

where α determines the error of our estimation. For our convenience, we fit $t(y)$ to a polynomial function in each phase separately before determining its odd and even parts.

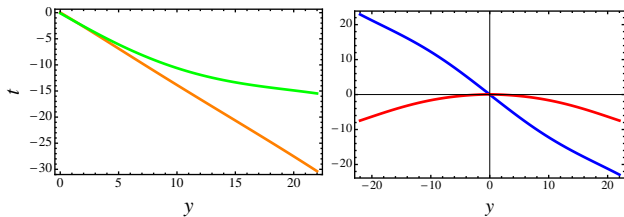


Figure 2: The final steps to measure the mirror symmetry range is presented for 4D lattice equal 4.34 (Left) $t(y)$ is plotted from fitting the modified SDRG results onto a 5th order polynomial function in each phase separately. Here the orange color corresponds to the localized and the green color to the delocalized phase (inverted to the positive y). (Right) The even and odd parts of function $t(y)$ is plotted separately.

In contrast to the $2 + \epsilon$ expansion theory which only predicts very small symmetry range, we find a significant range of mirror symmetry in 3D and higher. To see $2 + \epsilon$ expansion theory prediction for MSR, one can compute the scaling function g close to $d = 2$, i.e. for $\epsilon = d - 2 \ll 1$, we have the perturbative result:

$$\beta(g) \approx \epsilon - \frac{a}{g} + \dots, \quad (7)$$

or

$$\frac{1}{\epsilon} \int_{g(\ell)}^{g(L)} \frac{dg}{g - g_c} = \ln(L/\ell), \quad (8)$$

where $g_c = a/\epsilon$, ℓ is the mean-free path, and L is the system size; we assumed that we are on the metallic side, so $g(\ell) > g_c$. Let us denote $g(\ell) = g_o$, and $\delta g_o = g_o - g_c$. We obtain:

$$g(L) = g_c + \delta g_o (L/\ell)^\epsilon,$$

or

$$g(L) = F(L/\xi),$$

where $\xi = \ell \delta g_o^{-\nu}$, with $\nu = \epsilon^{-1}$, and the “metallic” branch of the scaling function of the form

$$F_{met.}(x) = g_c + x^\epsilon.$$

For large system sizes $g(L) \gg g_c$, and from the definition of the conductivity $g(L) = L^\epsilon \sigma$, we obtain

$$\sigma = \delta g_o^\mu,$$

with $\mu = \epsilon\nu$. Note also that the quantity δg_o measures the distance to the transition, i.e. $\delta g_o \sim (W - W_c)$, etc. Note also that for $\epsilon \ll 1$, this calculation is sufficient on the entire metallic side, since higher order terms in g^{-1} are negligible.

The same argument does not hold on the insulating side, since there $g(L)$ flows to zero, hence the higher order terms become large (in magnitude, as $\beta < 0$ there). Still, sufficiently close to the transition, the above “perturbative” form of the beta function remains sufficient, and we can repeat the same integration procedure (except now $g(L) < g_c$). We find

$$g(L) = g_c - (L/\xi)^\epsilon,$$

with $\xi = \ell |\delta g_o|^{-\nu}$. The corresponding “insulating” branch of the scaling function is

$$F_{ins.}(x) = g_c - x^\epsilon.$$

If we define the quantity $y = \pm x^\epsilon$, as usual, we can express both branches as parts of the same scaling function

$$F(y) = g_c + y.$$

This is an exact result for the scaling function in the regime where the perturbative form is valid.

Now we define the function

$$t(y) = \ln(g/g_c) = \ln(1 + \epsilon y). \quad (9)$$

Obviously, this function has mirror symmetry, only for $\epsilon y \ll 1$. In terms of the MSR, this means only a very small range. We can derive a more formal range using separating even and odd parts of $t(y)$. If we use $\alpha \ll 1$ as accuracy of our results in Eq. 6

$$\frac{t_{even}(y^*)}{t_{odd}(y^*)} = \alpha \longrightarrow \ln(1 + \epsilon y^*)(1 - \epsilon y^*) = \alpha \ln\left(\frac{1 + \epsilon y^*}{1 - \epsilon y^*}\right)$$

$$(1 + \epsilon y^*)^{\alpha+1} = (1 - \epsilon y^*)^{\alpha-1} \quad (10)$$

Solving the last equation gives two solutions $y^* = 0$ and $y^* = 2\alpha/\epsilon$. By putting back y^* in Eq. 9, and solving for g/g_c we find $MSR = 1 + 2\alpha$ which is a number of order of one.

V. THE ROLE OF k_{max} IN THE ACCURACY OF RESULTS

We introduced k_{max} as an upper cut-off for the number of bonds we store during SDRG decimation. Although this algorithm speeds up the running time (see Fig. 3), this idea is a heuristic argument and one expects an approximated results as we throw away more bonds no matter how weak are. One can look at this parameter as a control tool to adjust the accuracy of results as desired. In the extreme limits, when k_{max} approaches to N we get exact results and we loose significant information if we push it to very small numbers. In figure 4, we present the sensitivity of our results to the value of k_{max} for a cubic lattice. This figure does not necessarily imply anything about the best choice of k_{max} for other dimensions and even for larger system sizes. One safer approach might be to vary k_{max} as N increases and dimensionality changes.

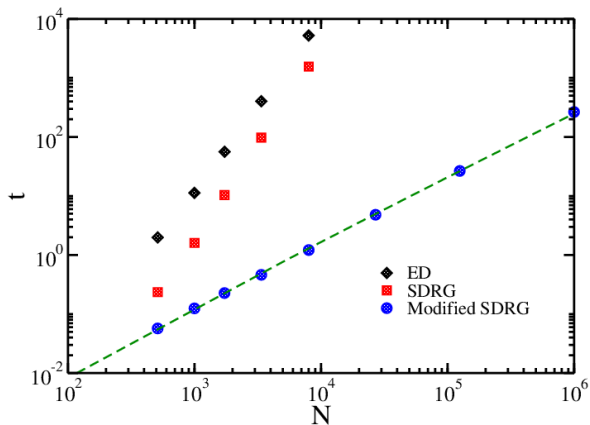


Figure 3: Computational time of the algorithm, t (in seconds in a 3.4GHz processor) for single realization of disorder as a function of the size of the cubic lattice, $N = L^3$, in a log-log scale for three different methods. The dashed line describes our theoretical prediction, $t \sim N \log N$. Here, the disorder value of the sample is $W = 17$.

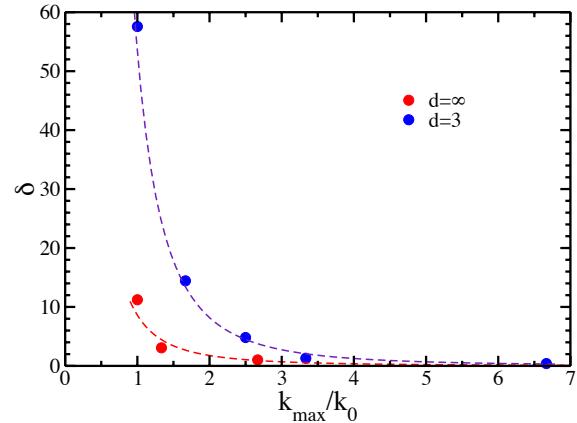


Figure 4: The produced error $\delta = \frac{|\nu - \nu_{exact}|}{\nu_{k_{max}^{act}}} \times 100$ in the computed critical exponent ν by varying k_{max} for 3D lattice and ER random graph. The same range of disorder strength from 8 to 24 is used for both models. The maximum system sizes in 3D lattice is $L = 20$ while For infinite dimensional limit, we used the ER random graph samples with $\langle k \rangle = 3.0$, the same range of disorder as cubic lattice, and site number $N = 3^{l_{ER}}$ where $l_{ER} = 4, 5, 6, 7$. Here, the k_{max} is normalized by the maximum initial coordination number, k_0 .

[1] M. A. Weiss, *Data Structures & Algorithm Analysis in C++* (Prentice Hall; 4 edition, 2013).